PHYSICAL REVIEW E **76**, 035401(R) (2007)

Electron attachment to C_7F_{14} and SF_6 in a thermally ionized potassium plasma

Su-Hyun Kim and Robert L. Merlino
Department of Physics and Astronomy, The University of Iowa, Iowa City, Iowa 52242, USA
(Received 22 March 2007; revised manuscript received 16 June 2007; published 14 September 2007)

Electron attachment to perfluoromethylcyclohexane (C_7F_{14}) and sulfur hexafluoride (SF_6) is studied in a Q machine which produces a thermally ionized potassium plasma at an electron temperature $T_e \simeq 0.2$ eV (2300 K). Negative ion formation is observed by Langmuir probe measurements of the reduction in electron density as electrons attach to C_7F_{14} to form $C_7F_{14}^-$ or to SF_6 to produce SF_6^-. In C_7F_{14} at a pressure $\sim 3 \times 10^{-5}$ Torr, a nearly electron-free plasma is formed with a residual electron-to-ion density ratio $n_e/n_+ < 10^{-4}$. Formation of the $C_7F_{14}^-$ negative ion was confirmed by the presence of the $C_7F_{14}^-$ electrostatic ion cyclotron wave mode in the power spectrum of current-driven plasma oscillations. Measurements of the negative ion-to-electron density ratio, n_-/n_e for different pressures in both C_7F_{14} and SF_6 indicate that for thermal electrons at 2300 K larger values of n_-/n_e are obtained in C_7F_{14} at a lower pressure than in SF_6.

DOI: 10.1103/PhysRevE.76.035401 PACS number(s): 52.27.Cm, 52.75.Xx

Negative ion plasmas are commonly found in various natural and technological environments including microelectronics plasma processing reactors, the D region of the ionosphere, the mesosphere, the solar photosphere, and in neutral beam sources [1]. When the "free" electron density n_e is $\ll n_-$, the negative ion density, so that $n_- \approx n_+$, the positive ion density, we have an "ion-ion" plasma with a number of interesting properties and uses, as discussed recently by Economou [1]. Negative ion plasmas are of particular interest in basic plasma physics due to the fact that many of the typical plasma phenomena (e.g., sheath formation, ambipolar electric fields, waves, and instabilities) are fundamentally altered in plasmas containing heavy negative charge carriers [2–5].

Sulfur hexafluoride, SF_6, has been widely used to produce plasmas with relatively large concentrations of negative ions. SF_6 (molecular weight 146) has a negative ion resonant capture peak at zero or near-zero electron energy, and thus is very efficient in attaching low energy electrons through the process $SF_6 + e \rightarrow (SF_6^-)^* \rightarrow SF_6^-$ [6]. For electron energies below 0.2 eV, the attachment cross section $\sigma_a^{SF_6}$ is $\sim 10^{-15}$ cm^2, so that negative ion plasmas with electron-to-positive ion density ratios, $n_e/n_+ \ll 1$, can be obtained at relatively low SF_6 pressures. For example, Sheehan and Rynn [4] found that at $P_{SF_6} \sim 2 \times 10^{-6}$ Torr, the electron density in a Q machine [7] plasma was reduced by a factor of 10. Sato reported an electron fraction relative to the positive ions in a Q machine, $n_e/n_+ \sim 10^{-4}$ for $P_{SF_6} \sim 5 \times 10^{-4}$ Torr [5]. Q machines are ideal negative ion sources [4,5] due to the low electron temperature, $T_e \approx 0.2$ eV, resulting from thermal ionization. Hot filament discharge plasmas, such as those used in multidipole devices [8], are also efficient negative ion sources, but the presence of much hotter electrons ($T_e \sim 1-5$ eV) as well as energetic ionizing electrons (tens of eV) leads to the production of SF_5^- and F^- as well as SF_6^- [6]. The "magnetic cusp cage," which confines energetic electrons and allows only cold electrons ($T_{e,\mathrm{cold}} \approx 0.2$ eV) to pass through the cage where they attach to SF_6, has also been used to produce negative ion plasmas [2,9]. Negative ion formation in hot filament discharges generally requires higher gas pressures than in Q machines.

An important goal in this field is to produce a large concentration of negative ions at as low a neutral gas pressure as possible in order to maintain low plasma collisionality. We investigated the formation of a negative ion plasma in a Q machine using C_7F_{14}, and compared the electron attachment efficiency of C_7F_{14} with that of SF_6 at different gas pressures under otherwise identical conditions. This comparison provides a direct inference of the relative thermal electron attachment rates of SF_6 and C_7F_{14} at $T_e = 2300$ K. The formation of a negative ion plasma in C_7F_{14} leads to the formation of a negative ion of mass m_- heavier than that of SF_6^- (146 amu) through the reaction $C_7F_{14} + e \rightarrow (C_7F_{14}^-)^* \rightarrow C_7F_{14}^-$ (350 amu). Such a plasma affords the possibility, e.g., of studying the charging of dust particles to *positive* potentials [10], as recently observed in the polar mesosphere [11].

Experiment. The setup is shown in Fig. 1. Potassium atoms from an atomic beam oven undergo surface ionization on a 6 cm diameter, electrically grounded tantalum hot plate (HP) which is heated by electron bombardment to $T_{HP} \approx 2300$ K. K^+ ions and thermionically emitted electrons emerge from the hot plate as a nearly fully ionized plasma and are confined radially by a uniform longitudinal magnetic field B = 0.25–0.4 *T*. The plasma is terminated by a cold end plate located ~ 1 m from the HP. The electron and ion temperatures are typically $\sim T_{HP}$, with $T_e \approx T_+ \approx 0.2$ eV, and the plasma density is in the range, $n_+ \sim 10^8 - 10^{10}$ cm^{-3}. The plasma potential, electron and ion densities, and the electron temperature were measured using planar Langmuir probes of diameter 2–4 mm.

Negative ion plasmas were produced by introducing

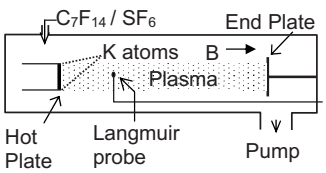

FIG. 1. Schematic of the experimental apparatus—a single-ended Q machine.

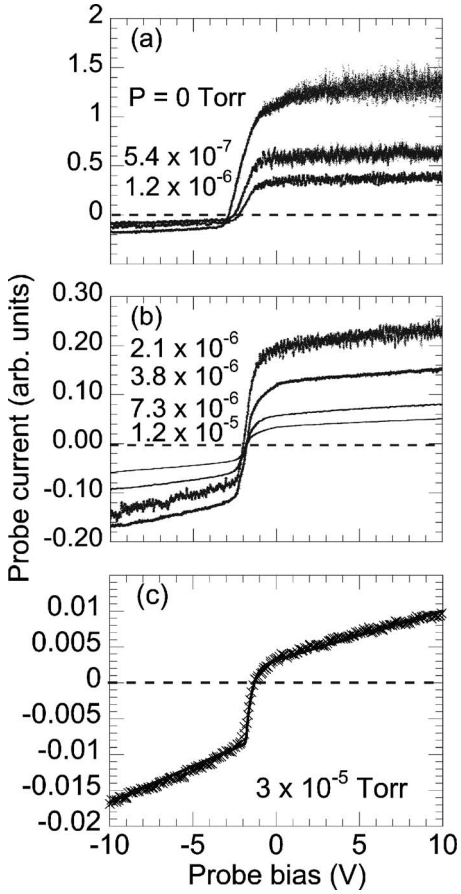

FIG. 2. Langmuir probe current-voltage (*I-V*) curves for various C_7F_{14} pressures. (a) Low pressures, (b) intermediate pressures, and (c) 3×10^{-5} Torr. Positive probe current is due to collection of electrons and negative ions, while negative probe current is due to the collection of positive ions. The uppermost curve in (a) corresponds to a plasma with no C_7F_{14} added. The solid curve in (c) is a theoretical probe fit to the experimental points.

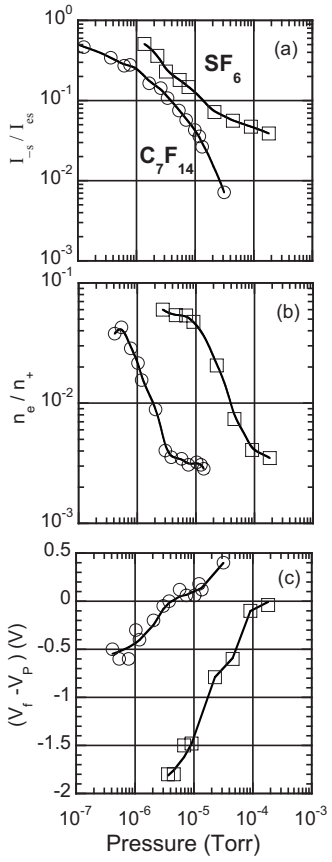

FIG. 3. Properties of negative ion plasmas formed in SF_6 (open squares) and C_7F_{14} (open circles). Ratio of the probe currents due to electrons and negative ions to the electron current in the absence of negative ions vs pressure. (b) Residual fractional electron concentration vs pressure. (c) Difference between the probe floating potential, V_f, and plasma potential, V_p, vs pressure.

C_7F_{14} vapor or SF_6 gas into the vacuum chamber (base pressure $\sim10^{-6}$ Torr). C_7F_{14} is a clear, colorless, odorless, stable liquid (density 1.78 g/cm^3) with a vapor pressure of 107 Torr at 25 °C. A flask containing about 100 ml of C_7F_{14} is connected to the main vacuum chamber with tubing and the vapor is leaked in using a fine needle valve. Absorbed gases in the C_7F_{14} are removed by pumping on the flask with a mechanical pump; this process is repeated several times. Since the ionization gauge gas sensitivity factor for C_7F_{14} was not available, a gas sensitivity factor $S_{C_7F_{14}}/S_{N_2}\approx6.3$ was estimated following the method of Hollanda [12]. No harmful effects on any vacuum components have been observed with the use of C_7F_{14}.

Results and discussion. Figure 2 shows a series of Langmuir probe *I-V* curves obtained for increasing pressures of C_7F_{14}. The probe was located on axis approximately 50 cm from the hot plate. Following the typical practice for probe *I-V* plots, the current due to the collection of the negative particles (electrons+negative ions), $I_-=I_e+I_n$, is shown as the *positive* current, while the current due to the collection of the positive ions, I_+, is shown as the *negative* current. The uppermost *I-V* curve in Fig. 2(a) was taken with no C_7F_{14} present. As the C_7F_{14} pressure, $P_{C_7F_{14}}$, was increased, I_- decreased as electrons became attached to the considerably less mobile $C_7F_{14}^-$ ions. The series of *I-V* curves in Figs. 2(a) and 2(b) shows that I_- and I_+ became comparable as $P_{C_7F_{14}}$ was increased, with I_+ exceeding I_- for $P_{C_7F_{14}}>7\times10^{-6}$ Torr. For $P_{C_7F_{14}}=3\times10^{-5}$ Torr [Fig. 2(c)], the attachment rate of electrons is so large that the negative probe current is due mostly to the collection of negative ions. The positive current now exceeds the negative current by about a factor of 4, since the positive ions are now the lighter species in the plasma.

A plot of the ratio I_{-s}/I_{es}, where I_{-s} is the total probe negative saturation current (due to the collections of electrons and negative ions) at a given value of pressure P, and I_{es} is the electron saturation current for P=0, is shown in Fig. 3(a) for both C_7F_{14} and SF_6. The SF_6 data were obtained from Langmuir probe measurements (similar to those shown in Fig. 2 using C_7F_{14}) when SF_6 was used. The comparison between the C_7F_{14} and SF_6 results shows that: (i) the effect of electron attachment is observed at lower pressures with C_7F_{14} compared to SF_6, (ii) higher pressures of SF_6 are required to produce comparable electron density reductions,

and (iii) larger reductions in electron density are observed in C_7F_{14}. Measurements of the ratio of the negative to positive saturation currents, I_{+s}/I_{-s} provide a rough estimate of n_e/n_+ and $n_-/n_+=1-n_e/n_+$ using $I_{+s}=en_+(kT_+/2\pi m_+)^{1/2}A_p$ and $I_{-s}=e[n_e(kT_e/2\pi m_e)^{1/2}+n_-(kT_-/2\pi m_-)^{1/2}]A_p$, where n_j, $j=(+,e,-)$ is the density of positive ions, electrons, and negative ions and A_p is the probe collection area. The n_e/n_+ values for C_7F_{14} and SF_6 are shown in Fig. 3(b). When $n_e/n_+<10^{-3}$, corresponding to the case of Fig. 2(c), it is difficult to obtain accurate values of n_e/n_+ from probe measurements [5]. In this case we used an iterative procedure to obtain a theoretical fit to the *I-V* curve in Fig. 2(c), first assuming $n_e/n_+=0$, and then obtaining an upper limit for n_e/n_+ based on the maximum tolerable deviation in n_e/n_+ consistent with the fit (solid curve). This procedure leads to an upper limit on n_e/n_+ of 5×10^{-5} at $P_{C_7F_{14}}=3\times10^{-5}$ Torr.

Figure 3(c) shows results of probe measurements of the difference, (V_f-V_P), between the probe floating potential V_f and the plasma potential V_p. For each *I-V* plot, the plasma potential was identified as the potential where the derivative of the *I-V* curve was a maximum. This result shows that as more and more electrons are attached to form negative ions (with increasing pressure), the plasma becomes more and more mass symmetric, and (V_f-V_P) becomes less and less negative. In the case of C_7F_{14}, (V_f-V_P) obtains *positive* values, since $m_+<m_-$, the positive ions are now the more mobile species, and $V_f>V_p$.

The $C_7F_{14}^-$ negative ions were identified by observations of the spectrum of electrostatic ion cyclotron (EIC) oscillations which are excited in the plasma due to a current-driven instability [13]. Similar observations were reported previously for negative ion plasmas in SF_6 [14–16]. An electron current was drawn along the magnetic field to a 1 cm diameter disk electrode which was located radially in the center of the plasma column and biased at a dc voltage above the plasma potential. In an electron/K^+ plasma, the instability produces electrostatic oscillations in the plasma density and potential at frequencies slightly above the K^+ ion cyclotron frequency, $f_{c,K^+}=eB/2\pi m_+$, as shown in Fig. 4(a). In this case, the fundamental and first harmonic modes appear at 165 and 340 kHz. At a magnetic field of 0.4 T, the ion cyclotron frequencies for K^+ and $C_7F_{14}^-$ are $f_{c,K^+}=156$ kHz and $f_{c,C_7F_{14}^-}=17.5$ kHz, respectively. Figure 4(b) shows the corresponding EIC oscillation spectrum with C_7F_4 at $P=6\times10^{-7}$ Torr. The K^+ fundamental and first harmonic EIC modes are shifted up to 230 and 450 kHz, and two low frequency peaks appear at 25 and 50 kHz, which correspond to the fundamental and first harmonic of the $C_7F_{14}^-$ EIC mode. Note that the EIC mode frequencies do not occur at the respective ion cyclotron frequencies, but at frequencies about 1.5 times the corresponding ion cyclotron frequencies. This is in line with calculations based on the theoretical dispersion relation for EIC waves in a plasma with positive ions, negative ions, and electrons [17], which predicts an upward shift in frequency of both positive ion and negative ion EIC modes as the fraction of negative ions increases. The observed frequency shift is consistent with that expected for the value of n_-/n_+ for $P\lesssim10^{-6}$ Torr. Further observations showed that the frequencies of both the light and heavy EIC

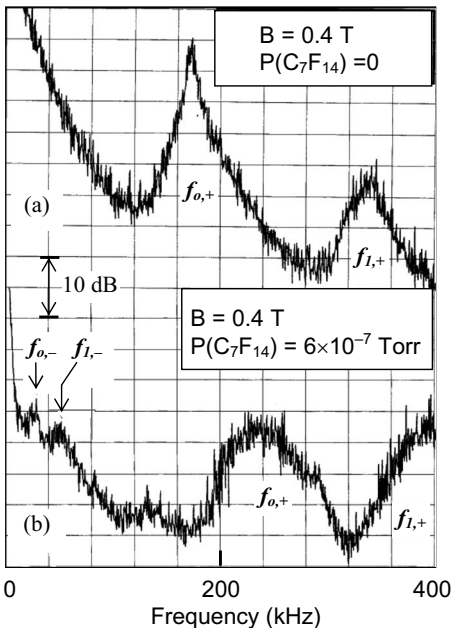

FIG. 4. Power spectra (0–200 kHz) of electrostatic ion cyclotron wave oscillations excited spontaneously in the plasma by drawing an electron current along the magnetic field, for B=0.4 T. (a) $P_{C_7F_{14}}=0$. (b) $P_{C_7F_{14}}=6\times10^{-7}$ Torr.

modes continued to increase as the fraction of negative ions increased. However, at $P\gtrsim2\times10^{-6}$ Torr, all EIC modes were quenched, probably due to the fact that the electron density was too low to sustain the critical current for wave excitation.

The present results indicate that at $T_e\cong0.2$ eV the rate constant for thermal electron attachment to C_7F_{14} is larger than that of SF_6. This conclusion appears to be in agreement with reported measurements of electron attachment cross sections and rate constants for SF_6 and C_7F_{14}. Using monoenergetic electron beams, Asundi and Craggs [18] measured electron attachment cross sections for both SF_6 and C_7F_{14} as a function of electron energy, E_e, and obtained maximum attachment cross sections of 1.3×10^{-15} cm^2 at $E_e=0.03$ eV for SF_6 and 7.5×10^{-15} cm^2 at $E_e=0.15$ eV for C_7F_{14}. These results were in qualitative agreement with the microwave cavity resonance measurements of Mahan and Young [19] of the rate constants for attachment of thermal electrons to SF_6 and C_7F_{14} at 300 K. Mahan and Young [19] also point out that an *increase* in the electron temperature led to a *decrease* in the rate of attachment to SF_6 while leaving the attachment rate to C_7F_{14} unchanged or slightly *increased*. The measurements of Mahan and Young [19] were in excellent agreement with subsequent work of Chen *et al.* [20] using pulse-sampling techniques. These latter measurements support the general conclusion of Asundi and Craggs [18] that the attachment cross section for C_7F_{14} peaks at a higher energy than that of SF_6. In 1995 Spanel *et al.* [21] reported measurements of the attachment rates of SF_6 and C_7F_{14} as a function of electron temperature using the flowing afterglow/Langmuir probe (FALP) method. To benchmark these results, we note that the Spanel *et al.* [21] measurements for SF_6 agree very well with those of Petrovic and Crompton

[22] using an electron density sampling technique. Spanel *et al.* found that the attachment rate for SF_6 decreased with increasing T_e while that for C_7F_{14} increased with increasing T_e. There have been further measurements indicating that at $E_e=0.2$ eV, the attachment cross section for C_7F_{14} was larger than that of SF_6. Christodoulides and Christophorou [23] reported results of a swarm study of electron attachment to C_7F_{14} which showed resonance maxima at 0.07 and 0.25 eV with cross section values of 114.7×10^{-16} and 64.6×10^{-16} cm^2, respectively. Their value of 59.7×10^{-16} cm^2 at 0.2 eV for C_7F_{14} should be compared with the value of 2.86×10^{-16} cm^2 at 0.2 eV reported by Christophorou and Olthoff [6] for SF_6. Within the measurement uncertainties, the value reported in Ref. [6] for SF_6 agreed with that of Braun *et al.* [24], who used the laser photoelectron attachment (LPA) method which is considered to be the most accurate technique to determine cross sections for SF_6. Braun *et al.* [24] also found that the cross section for the formation of SF_6^- decreased by five orders of magnitude over the range 1–500 meV.

We have performed additional measurements (to be presented in an extended publication) indicating that in our experiments at $T_e\cong0.2$ eV the average attachment cross section for C_7F_{14} is about a factor of 10 higher than that of SF_6. This estimate was based on Langmuir probe electron density measurements along the axis of the Q machine (the z coordinate). The electron density varied as $n_e(z)=n_e(0)\exp(-\alpha z)$, from which the inverse scale length α was determined for both C_7F_{14} and SF_6. Since electron losses due to diffusion are negligible in the Q machine compared to attachment losses, the average attachment cross section $\bar{\sigma}_a$ can be directly related to α as $\alpha=N\bar{\sigma}_a$, where N is the density of the attaching gas. The exponential decay of the electron density along the axis of the plasma column indicates that the $C_7F_{14}^-$ and SF_6^- negative ions are stable against autodetachment for times at least as long as it takes to travel the length of the plasma column which is $\sim$ milliseconds.

In conclusion, a negative ion plasma with $m_-\approx10m_+$ and a very low residual electron content ($n_e/n_+<10^{-4}$) has been produced by electron attachment to C_7F_{14} at a pressure $\sim10^{-5}$ Torr. Measurements comparing the effects of C_7F_{14} and SF_6 indicate that C_7F_{14} has a higher cross section for thermal electron attachment at 0.2 eV than SF_6. The relatively long lifetimes of the $C_7F_{14}^-$ and SF_6^- negative ions points to the importance of intramolecular vibrational relaxation (IVR) in stabilizing the excited intermediates against autodetachment [25].

ACKNOWLEDGMENTS

We thank R. Fisher, V. Nosenko, N. D'Angelo, and M. Miller for useful discussions and technical assistance. This work was supported by the U.S. Department of Energy under Contract No. DE-FG02-04ER54795.

[1] D. J. Economou, Appl. Surf. Sci. **253**, 6672 (2007); Z. Lj. Petrovic *et al.*, *ibid.* **253**, 6619 (2007).
[2] A. Y. Wong, D. L. Mamas, and D. Arnush, Phys. Fluids **18**, 1489 (1975).
[3] T. Intrator and N. Hershkowitz, Phys. Fluids **26**, 1942 (1983).
[4] D. P. Sheehan and N. Rynn, Rev. Sci. Instrum. **59**, 1369 (1988).
[5] N. Sato, Plasma Sources Sci. Technol. **3**, 395 (1994).
[6] L. G. Christophorou and J. K. Olthoff, J. Phys. Chem. Ref. Data **29**, 267 (2000).
[7] R. Motley, *Q Machines* (Academic, New York, 1975).
[8] R. Limpaecher and K. R. MacKenzie, Rev. Sci. Instrum. **44**, 726 (1973).
[9] N. Hershkowitz and T. Intrator, Rev. Sci. Instrum. **52**, 1629 (1981).
[10] S. H. Kim and R. L. Merlino, Phys. Plasmas **13**, 052118 (2006).
[11] M. Rapp *et al.*, Geophys. Res. Lett. **32**, L23821 (2005).
[12] R. Hollanda, J. Vac. Sci. Technol. **10**, 1133 (1973).
[13] R. W. Motley and N. D'Angelo, Phys. Fluids **6**, 296 (1963).
[14] D. P. Sheehan, Ph.D. thesis, University of California, Irvine, 1987 (unpublished).
[15] B. Song, D. Suszcynsky, N. D'Angelo, and R. L. Merlino, Phys. Fluids B **1**, 2316 (1989).
[16] N. Sato, in *A Variety of Plasmas*, edited by A. Sen and P. K. Kaw (Indian Academy of Sciences, Bangalore, 1989).
[17] N. D'Angelo and R. L. Merlino, IEEE Trans. Plasma Sci. **PS-14**, 285 (1986).
[18] R. K. Asundi and J. D. Craggs, Proc. Phys. Soc. **83**, 611 (1964).
[19] B. H. Mahan and C. E. Young, J. Chem. Phys. **44**, 2192 (1966).
[20] E. Chen, R. D. George, and W. E. Wentworth, J. Chem. Phys. **49**, 1973 (1968).
[21] P. Spanel, S. Matejcik, and D. Smith, J. Phys. B **28**, 2941 (1995).
[22] Z. Lj. Petrovic and R. W. Crompton, J. Phys. B **17**, 2777 (1985).
[23] A. A. Christodoulides and L. G. Christophorou, Chem. Phys. Lett. **61**, 553 (1979).
[24] M. Braun *et al.*, Eur. Phys. J. D **35**, 177 (2005)
[25] L. Suess, R. Parthasarathy, and F. B. Dunning, J. Chem. Phys. **117**, 11222 (2002).